Ocean Research 22(2): 69-80, 2000

Far-field Transport of Effluent Plumes Discharged from Masan Sea Outfalls

Young Do Kim‡, See Whan Kang*, Il Won Seo, Byung Cheol Oh*

School of Civil, Urban, and Geosystem Engineering, Seoul National University
San 56-1, Sillim-dong, Gwanak-gu, Seoul 151-742, Korea

**Coastal and Harbor Engineering Research Center, KORDI*
Ansan P.O. Box 29, 425-600, Korea

Abstract: A 3-D particle tracking model with normalized characteristic equations has been developed to predict the variation of near-field mixing characteristics and the far-field transport of the effluent plumes discharged from sea outfalls. The model was applied to the case study on the Masan sea outfall plumes discharged through a submerged multiport-diffuser. Numerical simulations of the effluent transport for 15 days which cover neap and spring tidal cycles in Masan Bay were conducted using fall velocities of the solid wastes and the initial plume characteristics obtained from normalized near-field characteristic equations. The results showed that time variations in near-field minimum dilutions with tidal ambient flow conditions are about 45~49. Most of the heavy particles in the effluent plumes were settled and deposited in the vicinity of the outfalls immediately, and the finer particles were transported eastwards 3 km away from the outfalls for 15 days. A similar depositional trend of contaminated sediment was also found during a recent field survey.

Key words: Near-field mixing, Far-field transport, Effluent plumes, Sea outfalls, Masan-Bay.

1. Introduction

The ocean outfall systems with submerged multiport diffuser are generally the most efficient way of maximizing the initial dilution of wastewater discharges. The wastewater contain solids which cover a wide range of particle dimensions from less than 0.1 mm to more than 3 cm, and of different natures such as floating matters, settling matters, colloid matters, and matters in solution (Neves and Fernando 1995). Some of them may not be removed through treatment plants before being discharged, because most ocean disposal systems just have screens for the coarse particles. After the initial mixing in the near-field by buoyant jet flow, the established wastefield is diffused by the oceanic turbulence as it drifts with the ocean currents. The tidal currents oscillate with an amplitude that is typically much greater than the residual mean. The wastefield may then wander in the vicinity of the diffuser for some time before being flushed away by the residual mean drift (Roberts 1999). Therefore, some of the solids contained in wastewater discharges are settled and accumulated around submerged diffusers during the far-field dispersive phase. The accurate prediction of physical dilution and stochastic transport of effluent constituents is required to assist in coastal resources management and to safeguard public health (Wood *et al.* 1993). The dispersion process under the flowing currents is three-dimensional in nature and particularly

‡Corresponding author.
E-mail : greendo@chollian.net Fax : +82-2-887-0349

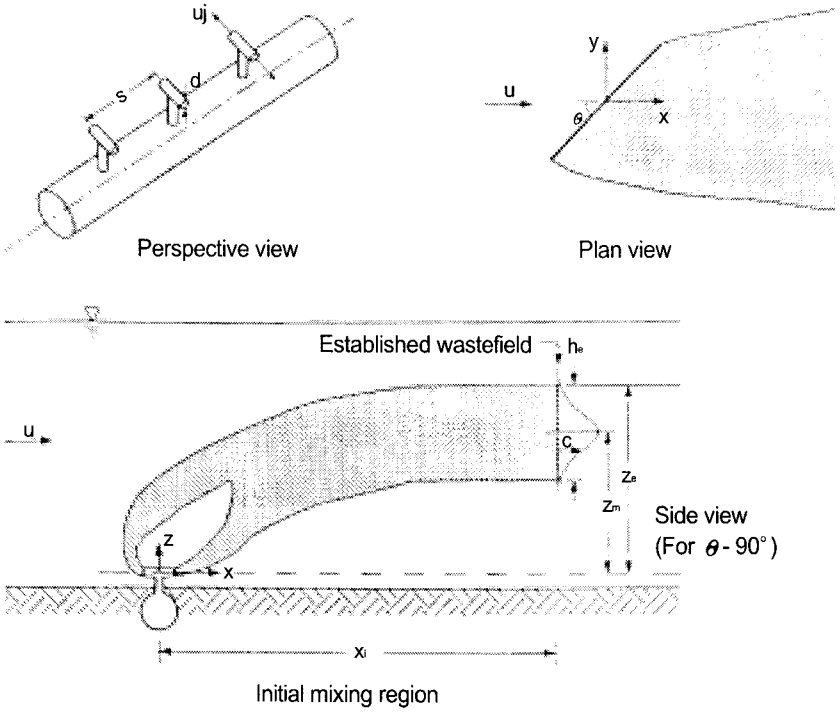

Fig. 1. The definition diagram of multiport diffuser(adapted from Roberts *et al.* 1989).

complex in the near-field region. Although many numerical studies on the dispersion of line plumes have been conducted previously, most of them deal with a 2-D simplified configuration of an infinite diffuser under perpendicular currents. Suh (1998) developed a 2-D Eulerian-Lagrangian model and semi-active particle tracking random walk model, and simulated surface discharged heat dispersion in coastal area. Seo and Cheong (1999) simulated dispersion processes in natural streams using a 2-D random-walk model, and showed that the error decreases as the number of grid increases and the number of particles in each grid increases.

Because of the various length and time scales associated with the transport of effluent plumes, both the near-field modeling and the far-field modeling are performed separately (NRC 1993). The problem with employing separate near and far-field models is treatment disability of interface between two fields. The far-field models can not resolve the near-field, and near-field models ignore any ambient sources or far-field return of pollution. This study is a subsequent work of Kang *et al.* (2000) which investigated the near-field initial mixing characteristics of the wastewater effluent discharged from Masan outfalls. In this paper, the far-field transport of the particles which were contained in wastewater effluents was investigated using the 3-D particle tracking model with normalized characteristic equations. This model can simulate initial mixing, advection, diffusion, and settling processes of the discharged particles. The results of model simulations were also compared with the recent field data collected from the outfall area in Masan Bay.

2. Theoretical Background

The discharge system as shown in Fig. 1 can be characterized by the source fluxes per unit diffuser length of volume, q, momentum, m, and buoyancy, b.

$$q = Q_0 / L, \quad m = u_j q, \quad b = g_0' q \tag{1}$$

where Q_0 is the total discharge flowrate, L is the diffuser length, u_j is the discharge velocity, and g_0' is the effec-

Table 1. Wastefield variables for near field characteristics.

	F ($\theta = 90°$, perpendicular)				F ($\theta = 0°$, parallel)			
	~0.1	0.1~1	1~10	10~	~0.1	0.1~1	1~10	10~
z_c / l_b	2.6		$2.5F^{-1/6}$		2.6		$2.6F^{-1/24}$	
h_c / l_b	1.8	2.0	$2.0F^{-1/8}$	$2.5F^{-1/6}$	1.8		2.0	
z_m / l_b	1.7	1.9	$1.9F^{-1/9}$	$1.5F^{-1/6}$	1.7	1.9		$1.9F^{-1/9}$
x_i / l_b	2.0	$8.5F^{1/3}$			2.0	$10F^{1/6}$		
$S_m qN / b^{2/3}$	0.97	$2.19F^{1/6}$-0.52			0.97		$1.25F^{1/9}$	
$w(x)$	1+0.17[(x / l_b) $F^{-1/3}$] 1/2L				$0.7x F^{-1/3}$			

tive acceleration due to gravity. Ambient stratification can be represented by the buoyancy frequency, N.

$$N = \left(-\frac{g}{\rho_a} \frac{d\rho}{dz} \right)^{1/2} \tag{2}$$

where ρ_a is the ambient density. Wright *et al.* (1982) defined three length scales as below,

$$l_q = q^2 / m, \quad l_b = b^{1/3} / N, \quad l_m = m / b^{2/3} \tag{3}$$

Flows can be assumed to be fully turbulent and independent of molecular viscosity and Reynolds number effects. Also, l_q / l_b is much less than one for the range of conditions typical of ocean outfalls, and can be neglected. For the line plume situation of closely spaced jets of low momentum flux, l_m / l_b and s / l_b both tend to be zero. Therefore, the established wastefield properties and the normalized dilution can be expressed by using the dimensional analysis, as below.

$$\frac{z_c}{l_b}, \frac{h_c}{l_b}, \frac{z_m}{l_b}, \frac{S_m qN}{b^{2/3}} = f(F, \theta) \tag{4}$$

where z_c is the height to top of wastefield, h_c is the wastefield thickness, z_m is the height to the minimum dilution or maximum concentration, S_m is the minimum dilution, x_i is the length of the initial mixing field, F is the Roberts Froude number, and θ is the ambient current angle to the diffuser axis. Roberts *et al.* (1989) conducted the experiments for a range of parameters typical of ocean wastewater outfalls. From these experimental data, the following relationships for prediction of near-field mixing characteristics can be derived as summarized in Table 1, where w is the wastefield width.

After initial mixing, when a pollutant is released into a turbulent coastal current, the processes contributing to the subsequent dispersion of the plume involve both an advective component, which is a transport process, and a diffusive component, which is a mixing process. Advection is the bulk transporting process for a plume element of diluted effluent which is processed by the mean component of current, whereas diffusion is the spreading process of a plume element as a consequence of mixing, such as molecular diffusion, turbulence and eddies associated with the currents on a wide range of length scales. A far-field model alone, which may resolve the density-exchange flow, does not always

Table 2. Comparison of possible ways of coupling near and far field models(adapted from Zhang 1995).

	I (a)	I (b)	Ⅱ	Ⅲ	Ⅳ
Freshwater Input Q	origin	origin	origin	NF	-
Loading Input M	origin	origin	NF	NF	NF
Trap Height	×	√	√	√	√
Gravitational Spreading	×	√	×	√	×
Freshwater Balance	√	√	√	×	√
Role of Near Field Model	Initial Calibration only	Used dynamically w/ control	Used dynamically w/o control	Used dynamically w/o control	Used dynamically w/o control

predict the correct trap height and initial dilution, and overpredicts plume widths due to poor horizontal resolution. Recently, Zhang and Adams (1999) proposed the four possible ways of coupling two field models as shown in Table 2. One major concern in ocean outfall modeling is whether the effluent plume will experience correct ambient temperature and light level in a stratified ocean, however the far-field model does not always predict the correct trap height. In addition to contaminant loadings, an effluent is also characterized by the momentum and the buoyancy of freshwater discharges. The simplest way of coupling near-field and far-field models is to introduce loadings in a far-field model at the position predicted by a near-field model.

In the transition region between the near-field and the far-field, the flowrate in the plume, Q_1, and the maximum centerline concentration of a constituent, C_1, are given by

$$Q_1 = S_a Q_0, \quad C_1 = C_0 / S_a \tag{5}$$

where S_a is the average dilution, and C_0 is the discharge concentration. The plume width, b_1, and thickness, h_1, are related by the following relationship, which simply states that the plume is now moving at the same speed as the ambient current.

$$Q_1 = U b_1 h_1 \tag{6}$$

For the case of a diffuser discharge, the plume width is very close to the length of the diffuser ($b_1 = L$). Eq. 6 can be used to determine the plume thickness. For the case of single-port discharges, the plume thickness depends on the residual plume buoyancy. As a first approximation, a thickness of one-tenth the discharge depth can be assumes, and Eq. 6 can be used to determine the plume width (Clark and Morriss 1991).

3. Mathematical Model

Particle tracking model

The σ coordinate transformed transport equation for a conservative tracer C can be written as (Kim *et al.* 2000),

$$\frac{\partial HC}{\partial t} + \frac{\partial UHC}{\partial x} + \frac{\partial VHC}{\partial y} + \frac{\partial \Omega C}{\partial \sigma} = \frac{\partial}{\partial x}\left(E_H H \frac{\partial C}{\partial x}\right) + \frac{\partial}{\partial y}\left(E_H H \frac{\partial C}{\partial y}\right) + \frac{\partial}{\partial \sigma}\left(\frac{E_V}{H}\frac{\partial C}{\partial \sigma}\right) \tag{7}$$

in which $H(=h+\eta)$ is the total water depth, h is the bottom topography, η is the water surface elevation, U, V, Ω are the velocity components in principal directions, x, y, σ coordinates, E_H, E_V are the eddy diffusion coefficients in horizontal and vertical directions, and the vertical coordinate σ is defined as positively upward from a fixed reference datum. Writing the right hand side as a pure second derivative, the σ coordinate transformed transport equation becomes (Kim *et al.* 2000),

$$\frac{\partial HC}{\partial t} + \frac{\partial}{\partial x}\left[\left\{U + \frac{1}{H}\frac{\partial E_H H}{\partial x}\right\}HC\right] + \frac{\partial}{\partial y}\left[\left\{V + \frac{1}{H}\frac{\partial E_H H}{\partial y}\right\}HC\right] + \frac{\partial}{\partial \sigma}\left[\left\{\frac{\Omega}{H} + \frac{1}{H}\frac{\partial}{\partial \sigma}\left(\frac{E_V}{H}\right)\right\}HC\right] = \frac{\partial^2}{\partial x^2}(E_H HC) + \frac{\partial^2}{\partial y^2}(E_H HC) + \frac{\partial^2}{\partial \sigma^2}\left(\frac{E_V}{H^2}HC\right) \tag{8}$$

Expressions in bracket are defined as a matrix form,

$$A = \begin{bmatrix} U + (1/D)\partial(E_H H)/\partial x \\ V + (1/D)\partial(E_H H)/\partial y \\ \Omega/H + (1/H)\partial(E_V/H)/\partial \sigma \end{bmatrix} \tag{9}$$

$$\frac{1}{2}BB^T = \begin{bmatrix} E_H & & \\ & E_H & \\ & & E_V/D^2 \end{bmatrix} \tag{10}$$

Therefore, the transport equation can become the Fokker-Planck equation (Kim *et al.* 2000), and the positions of particles, $X(t)$, can also be described by nonlinear Langevin equation (Zhang 1995),

$$\frac{dX}{dt} = A(X,t) + B(X,t)R_n \tag{11}$$

where R_n is a vector whose elements are independent random numbers with zero mean and unity standard deviation. The initial position of particles can be obtained from normalized characteristics equation as below, and Fig. 2 shows a schematic diagram of the concept on a particle tracking method.

$$x = x_i \tag{12}$$

$$y=[y_0-w(x_1)/2, y_0+w(x_1)/2] \quad (13)$$

$$z=[z_m-h_1/2, z_m+h_1/2] \quad (14)$$

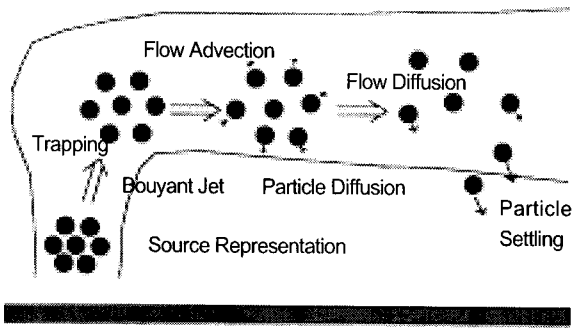

Fig. 2. Schematic diagram of particle tracking model.

There are two terms in each component of the deterministic force. The first one is the scaled velocity, and the second term is a pseudo velocity that makes a symmetrical distribution in physical domain by moving particles in the transformed grid (Zhang 1995). This combination of variables increases the complexity in interpreting results. Particle density is associated not only with concentration, but also with total water depth. After a certain period of time the particles will have spread widely enough so that the particles density distribution can be represented adequately by far-field grid cell concentration (Dimou 1992).

Hydrodynamic model

Hydrodynamic flow model is set up to compute the current velocity field. The continuity equation and three-dimensional Reynolds equations transformed to sigma coordinates with Boussinesq's and hydrostatic pressure assumptions can be written in the three dimensional form, as below (Blumberg and Mellor 1987),

$$\frac{\partial \eta}{\partial t}+\frac{\partial (HU)}{\partial x}+\frac{\partial (HV)}{\partial y}+\frac{\partial \Omega}{\partial \sigma}=0 \quad (15)$$

$$\frac{\partial (HU)}{\partial t}+\frac{\partial (HU^2)}{\partial x}+\frac{\partial (HUV)}{\partial y}+\frac{\partial (U\Omega)}{\partial \sigma}-\frac{\partial}{\partial \sigma}\left(\frac{K_v}{H}\frac{\partial U}{\partial \sigma}\right)$$

$$=fVH-gH\frac{\partial \eta}{\partial x}+F_x \quad (16)$$

$$\frac{\partial (HV)}{\partial t}+\frac{\partial (HUV)}{\partial x}+\frac{\partial (HV^2)}{\partial y}+\frac{\partial (V\Omega)}{\partial \sigma}-\frac{\partial}{\partial \sigma}\left(\frac{K_v}{H}\frac{\partial V}{\partial \sigma}\right)$$

$$=-fUH-gH\frac{\partial \eta}{\partial y}+F_y \quad (17)$$

in which K_v is the vertical eddy viscosity, f is the Coriolis' constant, g is the gravitational acceleration, and F_x, F_y are the horizontal viscosity terms. The K-l turbulence closure scheme is used to calculate vertical eddy viscosity and diffusivity.

$$\frac{\partial (Hq^2)}{\partial t}+\frac{\partial (HUq^2)}{\partial x}+\frac{\partial (HVq^2)}{\partial y}+\frac{\partial (\Omega q^2)}{\partial \sigma}-\frac{\partial}{\partial \sigma}\left(\frac{K_q}{H}\frac{\partial q^2}{\partial \sigma}\right)$$

$$=\frac{2K_v}{H}\left\{\left(\frac{\partial U}{\partial \sigma}\right)^2+\left(\frac{\partial V}{\partial \sigma}\right)^2\right\}-\frac{2Hq^3}{B_1 l}+F_q \quad (18)$$

$$\frac{\partial (Hq^2 l)}{\partial t}+\frac{\partial (HUq^2 l)}{\partial x}+\frac{\partial (HVq^2 l)}{\partial y}+\frac{\partial (\Omega q^2 l)}{\partial \sigma}-\frac{\partial}{\partial \sigma}\left(\frac{K_q}{H}\frac{\partial q^2 l}{\partial \sigma}\right)$$

$$=E_1 l\frac{K_v}{H}\left\{\left(\frac{\partial U}{\partial \sigma}\right)^2+\left(\frac{\partial V}{\partial \sigma}\right)^2\right\}-\frac{q^3 \tilde{W}}{B_1}+F_l \quad (19)$$

where q^2 is the two times the turbulent kinetic energy, l is the turbulence length scale, K_q is the vertical eddy diffusivity, F_q, F_l are the horizontal diffusivity terms, and $\tilde{W}$ represents the wall proximity function. The horizontal eddy viscosity and diffusivity can be obtained by the Smagorinsky formula that is given by the equation below (Davies *et al.* 1997).

$$K_h=C_s\Delta x\Delta y\left\{\left(\frac{\partial U}{\partial x}\right)^2+\frac{1}{2}\left(\frac{\partial V}{\partial x}+\frac{\partial U}{\partial y}\right)^2+\left(\frac{\partial V}{\partial y}\right)^2\right\}^{1/2} \quad (20)$$

where K_h is the horizontal eddy viscosity of horizontal viscosity terms, and C_s is the non-dimensional Smagorinsky's constant.

Numerical scheme

The governing equations of hydrodynamic model are solved numerically using the finite difference

method. The equations are discretized on a Arakawa C type staggered grid. The external mode portion of the model is two-dimensional, and a short time-step is used. The internal mode is three-dimensional, and a long time step is used. The external-mode calculation discretized by midpoint leap-frog approximation results in update information for surface elevations and depth averaged velocities. The internal-mode calculation separated into a vertical diffusion implicit time step which permit the use of finer vertical resolution, and an advection plus a horizontal diffusion explicit time step results in update information for velocities and turbulence quantities.

Interpolation and Boundary Conditions

In the C-grid, the U velocity components are defined at cell interfaces in the x direction, the V velocity components are defined at cell interfaces in the y direction, Ω components are defined on the top and bottom faces of cells, and other variables are defined at the center of cells. Interpolation accuracy can be improved by using extra interpolation points at neighboring layers, i.e., the one above or the one below the current layer depending on the relative elevation of the particle in the layer. Using the values from a neighboring layer brings the total number of nearest points to eight. Again, this interpolation can be done in a consecutively linear way (Kim *et al.* 2000).

Particles may encounter different types of boundary such as land, open, free surface, and bottom boundaries. Land and free surface boundaries are usually treated as non-flux boundaries where particles crossing the boundaries are reflected. Open boundaries are usually treated as flushing boundaries where a zero concentration boundary condition may be specified. Thus, particles crossing an open boundary are taken out of the domain. This approach assumes that open boundary has been chosen far enough away from the sources to minimize the possible contribution from returning pollutants.

4. Model Application

Masan-Jinhae Bay, a semi-enclosed bay with a narrow opening through Gadeokdo channel to open sea, is located in the southeastern part of Korea. The length scale along the North-South bay-axis is about 25 km, and the width along East-West direction is about 25 km. The total bay area is approximately 497 km^2 with the mean water depth of 15-20 m and the maximum depth of 50 m between Jamdo and Geojedo. Based on the field observations, there are strong semi-diurnal tidal currents along the relatively deep channel and at the bay mouth while very weak currents are present in the inner bay near Masan (Kang *et al.* 1989). As a part of the efforts for water quality improvement in Masan Bay, Masan-Changwon municipal wastewater treatment plants with the primary treatment has been in operation since 1993 with the treatment capacity of 280,000m^3/day. The Masan outfalls shown in Fig. 3 are located off the coast of Masan city and in Masan Bay.

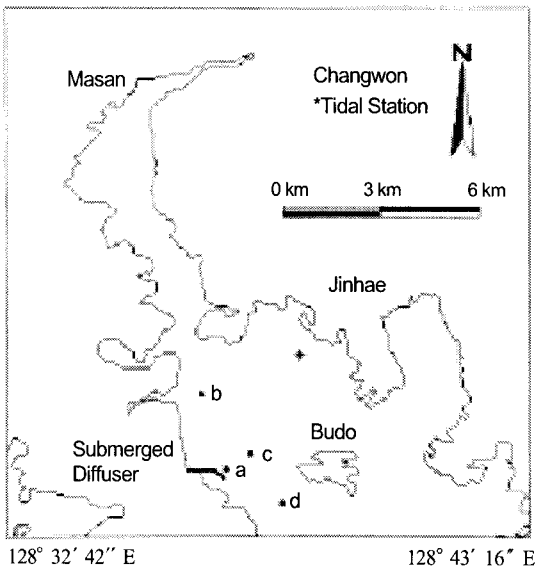

Fig. 3. Location map of the submerged ocean outfalls of Masan-Changwon POTW(a, b, c, d : field survey sites of deposited sediments).

The proposed hydrodynamic model was adopted to simulate the tidal currents with horizontal rectangular grids (Fig. 4). Based on field observations of Kang *et al.* (1993), the water elevation at the open boundary was prescribed with 4 major tidal constituents (M_2, S_2, K_1, O_1) during spring and neap tides, and performance was compared with the available observed data (Fig. 5). Fig. 6 shows the residual currents at surface and bottom layers which make differences in the streaklines of particles trapped at the thermocline depth. Field measure-

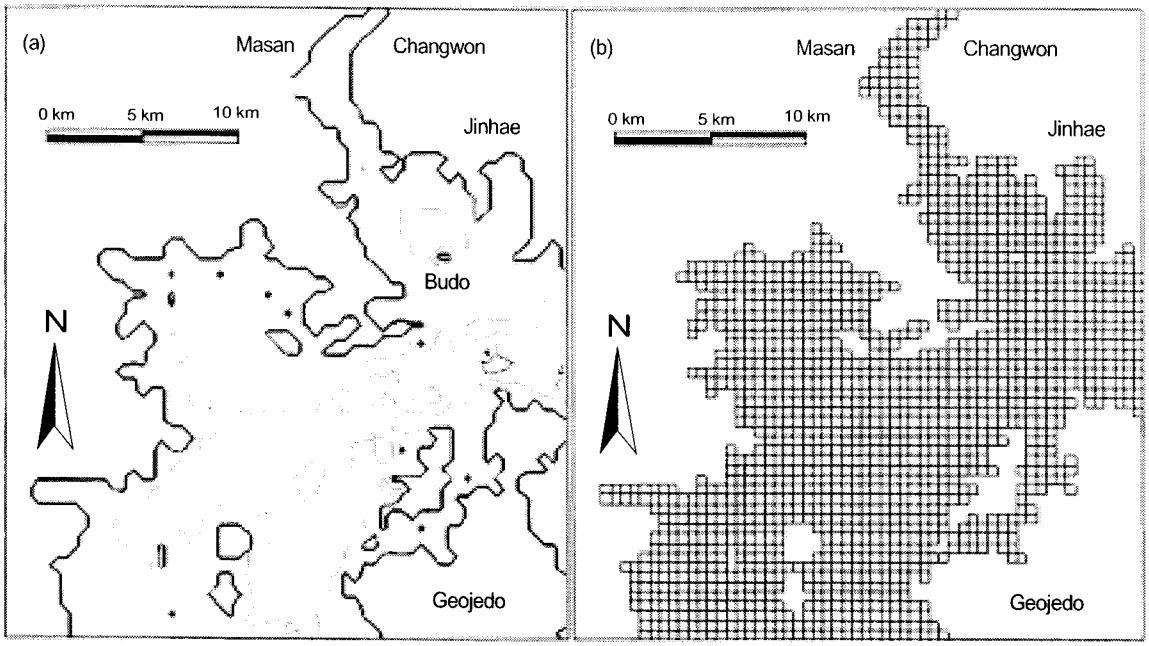

Fig. 4. Depths and grid system around Masan-Jinhae Bay.

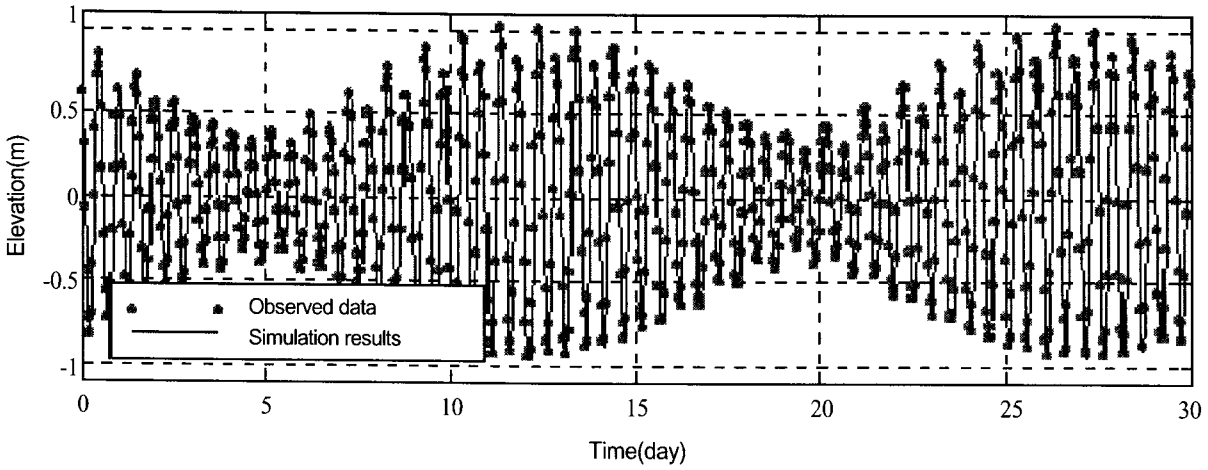

Fig. 5. Comparing the tidal elevation results with observed data.

ments of ambient conditions at the Masan outfalls site and its vicinity were conducted for two seasons, in the summer of 1998 and in the winter of 1999. They included vertical and horizontal distributions of temperature and salinity measurements by CTD. Fig. 7 shows vertical profiles of temperature and salinity in the summer and winter seasons that were used as input data of the model simulations for typical seasonal cases of summer and winter.

The near-field initial dilution of the outfall discharges depends primarily on the discharge, diffuser length, the depth of discharge, and the ambient conditions of current and density. Most geometry conditions of diffuser are constant, and if quasi-steady discharging conditions can be assumed, periodic ambient flow conditions may have significant effect on near-field dilutions. Fig. 8 shows time variations of near-field dilu-

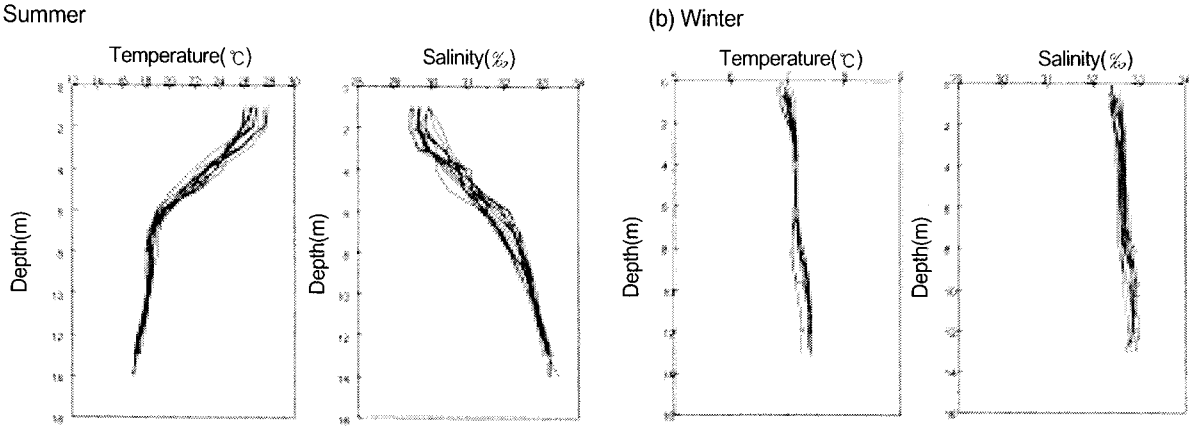

Fig. 6. Temperature and salinity profiles measured at the Masan outfalls site.

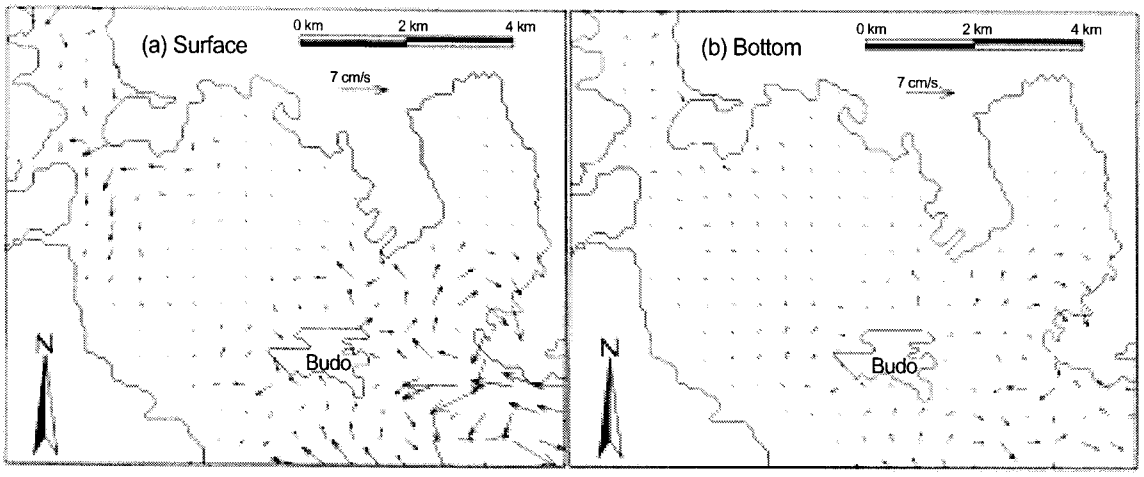

Fig. 7. Residual currents at surface and bottom layer.

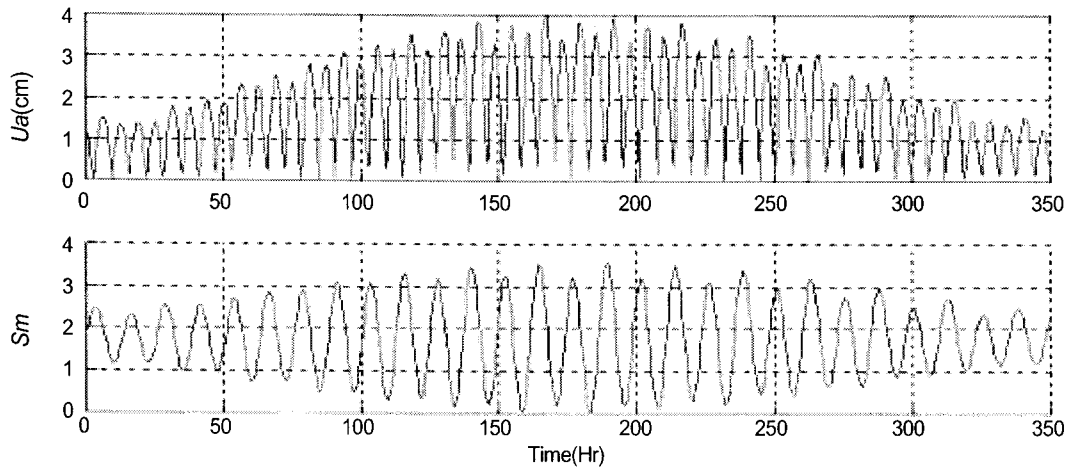

Fig. 8. The Variation of minimum dilution with tidal ambient current.

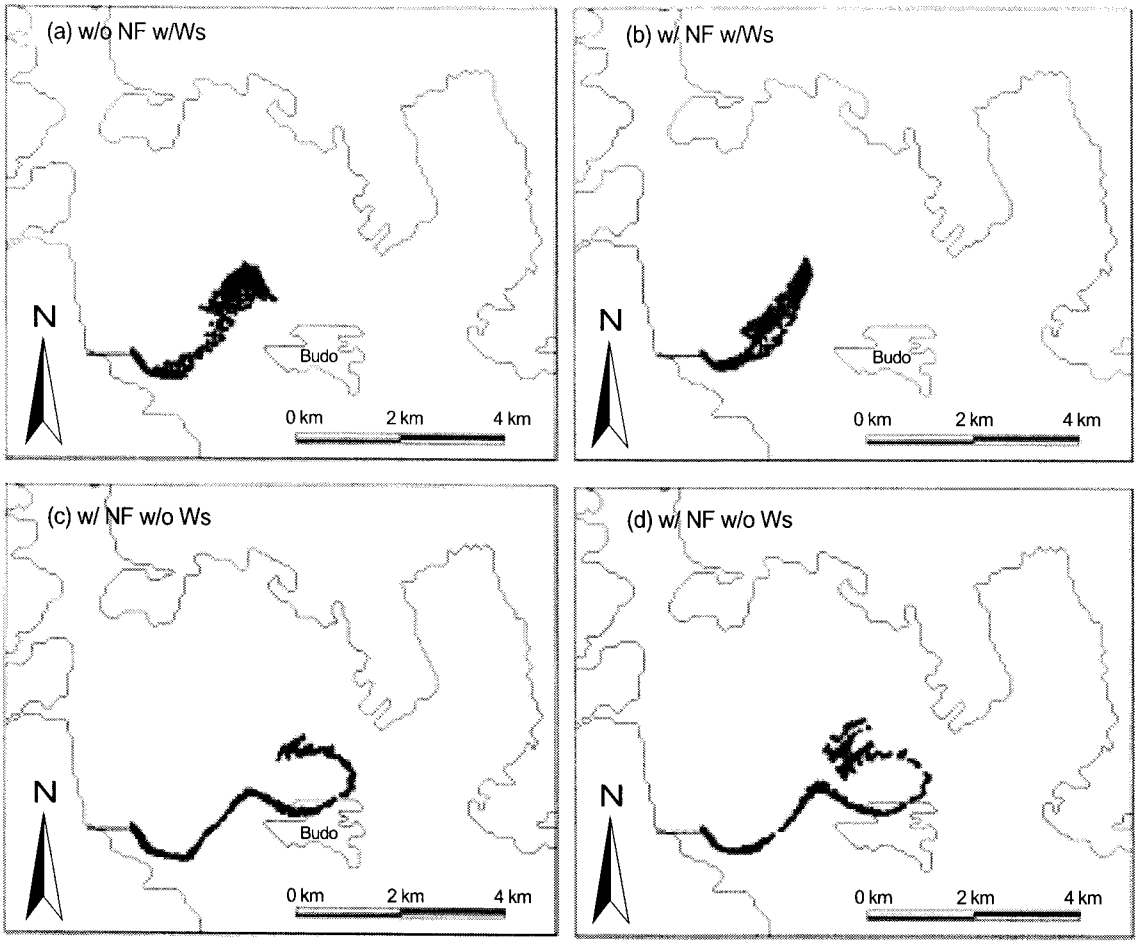

Fig. 9. Streaklines of particle at the end of near field.

tions with tidal ambient flow conditions, including a spring tide and a neap tide in Masan Bay. Kim *et al.* (2000) predicted a minimum dilution of about 40 at Masan outfalls by UM model for existing discharge records between 1994 and 1996, which is similar to the present study.

Fig. 9 shows particle streaklines trapped at thermocline with or without near-field calculations and fall velocities. Variations of the particle initial position by the near-field mixing do not affect only near-field characteristics, but also affect far-field transport with settling phenomenon of particles. Fig. 10 shows concentration profiles of settled and total particles considering the fall velocities. The number of introduced particles at each time step is 100, and the distributions of fall velocity are 10^{-5}~10^{-3} m/s, which is similar to EPA(1988) reports about the fine-grained sediment discharged from diffuser with the primary treatment. A similar depositional trend of contaminated sediment was also found in Table 3 from the recent field survey of Kwon and Lee (1998).

Table 3. Field survey data of deposited contaminants (adapted from Kwon and Lee 1998).

Site	Zn	Pb	Cd	Ni	Cu	Cr	Hg
a	305.1	46.8	2.73	34.9	54.9	57.6	0.18
b	243.9	34.4	0.98	23.3	46.3	47.6	0.15
c	148.2	22.9	0.42	24.3	27.4	42.6	0.10
d	127.0	30.0	-	19.0	24.7	36.7	0.08

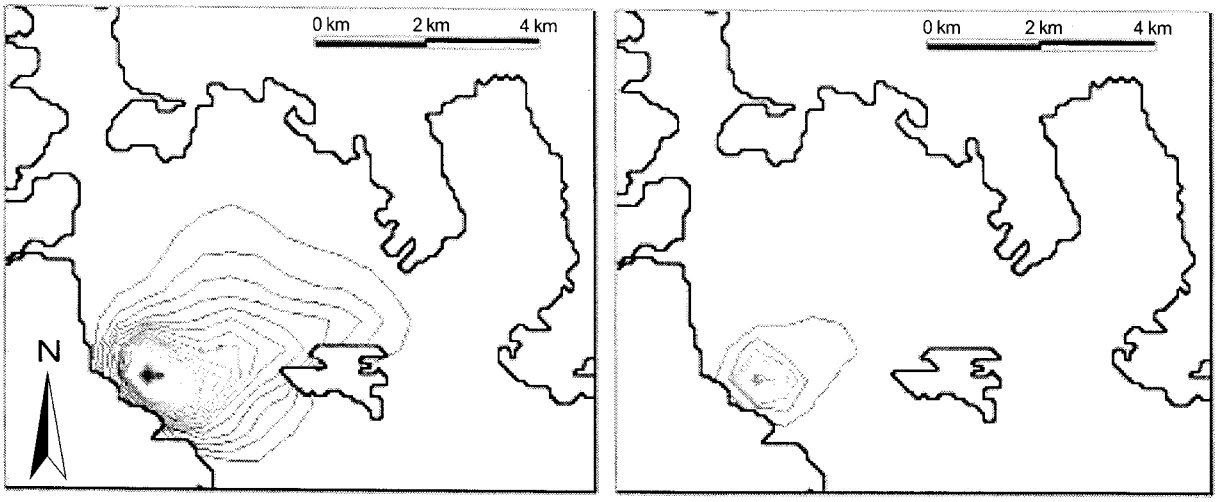

a) total particles b) settled particles

Fig. 10. Cencentration profiles of total and settled particles(contour lines : 15% of hourly discharged particles).

5. Conclusions

A 3-D particle tracking model with normalized characteristic equations has been developed to predict the variation of near-field mixing characteristics and the far-field transport of the effluent plumes discharged from sea outfalls. The model was applied to the case study of Masan sea outfall plumes discharged through a submerged multiport-diffuser. The results show that most of the heavy particles in the effluent plumes were settled and deposited immediately in the vicinity of outfalls. The finer particles were transported 3 km eastwards from the outfalls during the 15 days. The similar depositional trend of contaminated sediment was also found from the recent field survey. To predict water quality and sediment quality in the Masan sea outfall area, further works are needed for far-field modeling considering biological and chemical conversions, sedimentation, and final fate of the discharged particles.

Acknowledgments

This work was conducted at Seoul National University and Korea Ocean Research and Development Institute as a part of the National Environmental Technology R&D Project supported by the Ministry of Environment. We express our thanks to Dr. H. S. Choi and an anonymous reviewer for their reviews.

List of symbols

b	buoyancy fluxes per unit diffuser length
b_1	plume width
C	conservative tracer
$C_{0,}$	discharge concentration
C_1	maximum centerline concentration of a constituent
C_s	Smagorinsky's constant
E_h	horizontal eddy diffusion coefficient
E_v	vertical eddy diffusivity
f	Coriolis' constant
F	Roberts Froude number
F_x, F_y	horizontal viscosity terms
g	gravitational acceleration
g_0'	effective gravitational acceleration
h	bottom topography
h_1	plume thickness
h_2	thickness of the wastefield
H	total water depth
η	water surface elevation
K_H	horizontal eddy viscosity
K_q	vertical eddy diffusivity in transport equation for turbulence characteristics

K_v	vertical eddy viscosity
l	turbulence length scale
l_q, l_l, l_m	characteristic mixing length scale
L	diffuser length
m	momentum fluxes per unit diffuser length
N	buoyancy frequency
q	volume fluxes per unit diffuser length
q^2	twice turbulent kinetic energy
Q_o	total discharge flowrate
Q_1	flowrate in the plume
θ	angle of between ambient current and the diffuser axis
R_n	random numbers
ρ	density
ρ_a	ambient density
S_a	average dilution
S_m	minimum dilution
u_j	discharge velocity
U, V, Ω	velocity component at σ transformed coordinate
w	wastefield width
$\tilde{W}$	wall proximity function
x, y, σ	σ transformed coordinate
x_f	length of the initial mixing field
z_u	height to top of wastefield
z_m	height to the minimum dilution

References

Blumberg, A. F. and G. L. Mellor. 1987. A description of a three-dimensional coastal ocean circulation model. In *Coastal and Estuarine Sciences* 4, American Geophysical Union, 1-16.

Clark, B. J. and J. M. Morriss. 1991. Wastewater Engineering, Treatment, Disposal, and Reuse. 3rd ed., McGraw-Hill Inc., Singapore.

Davies, A. M., J. E. Jones, and J. Xing. 1997. Review of recent developments in tidal hydrodynamic modeling. I: Spectral models, II: Turbulence energy models. *J. of hydr. Engrg., ASCE*, 123(4), 278-292.

Dimou, K. 1992. 3-D hybrid Eulerian-Lagrangian / particle tracking model for simulating mass transport in coastal water bodies. Ph.D. dissertation, Depart-ment of Civil and Environmental Engineering, MIT.

EPA. 1988. Boston harbor wastewater conveyance system. Vol II. EPA. Region I. Boston, Massachusetts.

Neves, M. J. and H. J. S. Fernando. 1995. Sedimenta-tion of particle from jets discharged by ocean outfalls: a theoretical and laboratory study. *Wat. Sci. Tech.*, 32(2), 133-139.

NRC 1993. Managing wastewater in coastal urban areas. National Academy Press, Washington, D.C.

Kang, S. W. *et al.* 1993. A study on water quality management of enclosed coastal seas (I). KORDI Report, BSPN 00205-613-2.

Kang, S. W., S. H. You, and J. Y. Na. 2000. Near-field mixing characteristics of submerged effluent discharges. *Ocean Research*, 22(1), 45-56.

Kim, C.S., I. W. Seo, and M. H. Park. 2000. Dilution analysis of wastewater discharged through submerged multiport diffuser of Masan-Changwon W.T.P. *J. Kor. Soc. Civil Engrs.*, 20(2-B), 211-221.

Kim, Y. D., S. W. Kang, I. W. Seo, and B. C. Oh. 2000. Transport of submerged effluent discharges predicted by a three-dimensional particle tracking model. *J. Kor. Soc. Civil Engrs.*, 20(6-B), 843-852.

Kwon, Y. T. and C. W. Lee. 1998. Heavy metals contamination in coastal sediments by the large discharge from wastewater treatment plant. *J. Kor. Soc. Mar. Envir. Engrg.*, 1(1), 83-92.

Roberts, P. J. W. 1999. Modeling Mamala bay outfall plumes. I: Near field, II: Far field. *J. Hydr. Engrg., ASCE,* 125(6), *564-583.*

Seo, I. W. and T. S. Cheong. 1999. Modeling of transverse mixing in natural streams using 2-D random-walk model. *J. Kor. Wat. Resrc. Assoc.*, 32(2-B), 211-221.

Suh, S. W. 1998. Thermal dispersion analysis using semi-active particle tracking in near field combined with two-dimensional Eulerian-Lagrangian far field model. *J. Kor. Soc. Coast. Ocean Engrg.*, 10(2), 73-82.

Wood, I. R., R. G. Bell, and D. L. Wilkinson. 1993. Ocean disposal of wastewater. World Scientific, Singapore.

Wright, S. J., D. T. Wong, R. B. Wallace, and K. E. Zimmerman. 1982. Outfall diffuser behavior in stratified ambient fluid. *J. Hydr. Div., ASCE*, 108(HY4), 483-501.

Zhang, Z. Y. 1995. Ocean outfall modeling - Interfacing near and far field models with particle tracking method. Ph.D. dissertation, Department of Civil and

Environmental Engineering, MIT.
Zhang, X. Y., and E. E. Adams. 1999. Prediction of near field plume characteristics using far field circulation model. *J. Hydr. Engrg., ASCE*, 125(3), 233-241.

Received Oct. 30, 2000
Accepted Dec. 11, 2000